Fire retardancy of ethylene vinyl acetate/ultrafine kaolinite composites

Marcos Batistella, Belkacem Otazaghine, Rodolphe Sonnier, Anne-Sophie Caro-Bretelle, Carlos Petter, José-Marie Lopez-Cuesta

Fire retardancy of ethylene vinyl acetate/ultrafine kaolinite composites

Marcos Batistella [a,b], Belkacem Otazaghine [a], Rodolphe Sonnier [a,*], Anne-Sophie Caro-Bretelle [a], Carlos Petter [b], Jose-Marie Lopez-Cuesta [a]

[a] Ecole des Mines d'Alès, Centre des Matériaux (C2MA) – Pôle Matériaux Polymères Avancés, 6 Avenue de Clavières, 30319 Ales Cedex, France
[b] Universidade Federal do Rio Grande do Sul, Av. Bento Gonçalves, 8500 Porto Alegre, RS, Brazil

A B S T R A C T

The flame retardant effect of ultrafine kaolinite in Ethylene Vinyl Acetate copolymer (EVA) was studied and compared to that conferred by aluminum trihydrate (ATH). The thermal degradation and flammability of EVA composites were evaluated up to 60 wt% filler loading. Thermogravimetric (TG) and cone calorimeter analyses showed a higher decomposition temperature range and an improved FR performance for EVA/kaolinite composites in comparison to EVA/ATH composites. For a loading of 35 wt%, the peak of heat release rate (pHRR) of EVA/kaolinite was reduced by 55% compared to EVA/ATH. Moreover, we observed that kaolinite leads to a significant intumescent behavior during cone calorimeter tests. Finally, the rheology in the molten state of the different samples was studied and viscosity seems to play an important role on the fire retardancy of EVA/kaolinite composites.

Keywords:
Kaolinite
ATH
EVA
Flame retardancy

1. Introduction

Fire behavior of Ethyl Vinyl Acetate (EVA) copolymer has been extensively studied [1–9]. Many systems were proposed in the literature: halogenated compounds, phosphorated compounds and mineral fillers (micro and nanoparticles) [1,2,9–12]. Among those fillers, ATH is the most used flame retardant for EVA, particularly in the wire and cable industry. The dilution of fuel gases by water released by ATH above 200 °C and the associated endothermic effect are the most important mechanisms that improve the flame retardancy of the composites. Nevertheless, the high level of incorporation (at least 60 wt%) leads to a reduced flexibility, elongation at break and causes problems of processability. Mainly in combination with hydrated minerals, the use of clays as constituents of the flame retardant systems has been increasingly investigated. Recently many studies have involved the use of organically modified montmorillonite (oMMT), talc, halloysite or sepiolite as flame retardants or constituents of flame-retardant systems [5,7,11,13–18].

Other mineral fillers have been proposed to substitute ATH. The comprehensive study of Hull et al. [19] details the heat absorption of various hydrated fillers like calcium hydroxide, hydromagnesite, huntite and some others. In all cases, the main contribution to the heat absorption is the endothermic effect. Therefore, using hydrated fillers should be more efficient than inert fillers. But mineral fillers could act through other effects than heat absorption.

Other minerals, like kaolinite have received less attention. Kaolinite is an aluminosilicate with theoretical formula $Al_2Si_2O_5(OH)_4$ and basal interlayer space of 7.1 Å. Kaolinite is a 1:1 or TO type clay mineral, since it is formed by combining sheets of SiO_4^{4-} tetrahedra (T) and $Al(OH)_6^{3-}$ octahedra (O), in 1:1 proportion. The lamella remain attached to each other because they share common oxygen atoms, giving rise to the structure of the clay mineral [20,21]. It is widely used as paper filler and coating pigment. At the best of our knowledge, kaolinite is not widely used in polymer industry and few studies dealt with its use in polymers for mechanical or fire reaction purposes [22–25]. Therefore, in this study, the flame retardant effect of an ultrafine kaolinite in EVA was studied and compared with the most used filler in wire and cable industry: ATH.

Table 1 compares the temperature of decomposition, the water release and the associated endothermic decomposition energies for Kaolinite and ATH.

2. Materials and methods

Kaolinite (Paralux) used in this study from Brazilian deposits was supplied by Imerys. After mineralurgical treatments, a high

* Corresponding author.
E-mail address: rodolphe.sonnier@mines-ales.fr (R. Sonnier).

Table 1
Decomposition temperature and water release of kaolinite and ATH.

	Temperature of decomposition (°C)	Water release (%)	Energy of decomposition (J/g)
ATH Apyral 22	200–300	30	1054
Kaolinite	550–600	14	650 [26]

specific surface area was achieved: 14.2 ± 0.3 $m^2.g^{-1}$ (Brunauer–Emmett–Teller (B.E.T) method, using N_2 as adsorbed gas at 77 K on a Beckman Coulter SA3100 instrument). The average particle size (d_{50}) of kaolinite obtained by laser particle-size analysis (Coulter LS230) was estimated around 0.8 μm. Alumina hydroxide was supplied by Nabaltec Apyral 22, with a mean diameter of 12 μm and a specific surface area of 2 $m^2.g^{-1}$. This is a precipitated aluminum trihydrate which is commonly used for EVA in cable industry, mainly for the bending part of the cable. The EVA was Alcudia PA440 from Repsol and contained 28 weight-% of vinyl acetate.

2.1. Preparation of EVA composites

Compositions were extruded using a co-rotating twin-screw extruder (Clextral BC21 twin-screw extruder (Firminy, France), standard profile, length = 1200 mm, speed = 250 rpm, screw diameter = 20 mm, T = 120 °C–160 °C). The obtained pellets were injection molded (Krauss Maffei KM 50 t, T = 140–160 °C, mold temperature = 30 °C) to obtain square specimens (100 × 100 × 4 mm^3).

2.2. Characterization

Thermogravimetric analysis (TGA) was carried out on 10–12 mg samples at 10 °C.mn^{-1} from 50 to 800 °C under nitrogen or air flow using a Perkin–Elmer Pyris-1 TGA. A Scanning Transmission Electron Microscopy (FEI Quanta 200 SEM) was used to study the morphology of the samples. All images were obtained under high vacuum at a voltage of 15.0 kV. The cone calorimeter experiments were carried out using a Fire Testing Technology apparatus with an irradiance of 50 $kW.m^{-2}$, according to ISO 5660 standard. PCFC analysis was carried out according to the method A (anaerobic pyrolysis) of the ASTM D7309 using a FTT apparatus with a heating rate of 1 °C.s^{-1}, the maximum pyrolysis temperature was 750 °C and the combustion temperature was 900 °C (corresponding to complete combustion). The flow in combustor was a mixture of O_2/N_2 20/80 at 100 $cm^3.min^{-1}$ and the sample weight was 2 ± 0.5 mg. Viscosity measurements were carried out in dynamic mode at 160 °C using 0.5% strain and a frequency ranging from 10^{-1} s^{-1} to 10^2 s^{-1} (ARES, Rheometric Scientific). All samples were characterized in triplicate and mean values are showed.

3. Results and discussion

3.1. Cone calorimeter results

The Heat release Rate (HRR) and Mass Loss rate (MLR) curves for the composites are shown in Figs. 1 and 2 and complete results are shown in Table 2. As expected, pHRR is clearly reduced when the fillers are added to the polymer. These results show that the weight percentage of ATH must be at least 60 wt% in order to reach a significant improvement in fire retardancy in terms of pHRR (<300 $kW.m^{-2}$). Despite a lower amount in water (around 15 wt%) and higher temperatures for water release, EVA/kaolinite show a better flame retardancy than EVA/ATH. Even for 20 wt% of kaolinite, the samples show a significant decrease in pHRR. A loading of 35 wt % is enough to achieve a pHRR lower than 300 $kW.m^{-2}$.

Mass loss rate curves (Fig. 2) show the same tendencies since no flame inhibition effect is expected for both fillers. MLR and HRR are related through the Effective Heat of Combustion (EHC). The combustion efficiency (defined as the ratio between the effective heat of combustion in cone calorimeter and the heat of complete combustion measured in PCFC) is similar for all composites ($\chi = 1 \pm 0.1$). It means that the combustion is close to be complete (gases from pyrolysis are fully oxidized in the flame). Therefore, the only differences in EHC between EVA/kaolinite and EVA/ATH composites are due to the release of non-combustible gases. EHC values for EVA/ATH decrease as a function of filler loading, which confirms the influence of water release (fuel dilution). Since water release from kaolinite occurs during the test (as shown below), EHC does not change significantly (except for K60) because kaolinite releases only 14 wt% of water in the range 550–600 °C. This temperature range and the limited amount of water released could not explain the very good performances of EVA/kaolinite composites.

The Total Heat release (THR) is similar for both fillers containing composites and decreases in proportion to the filler content. The

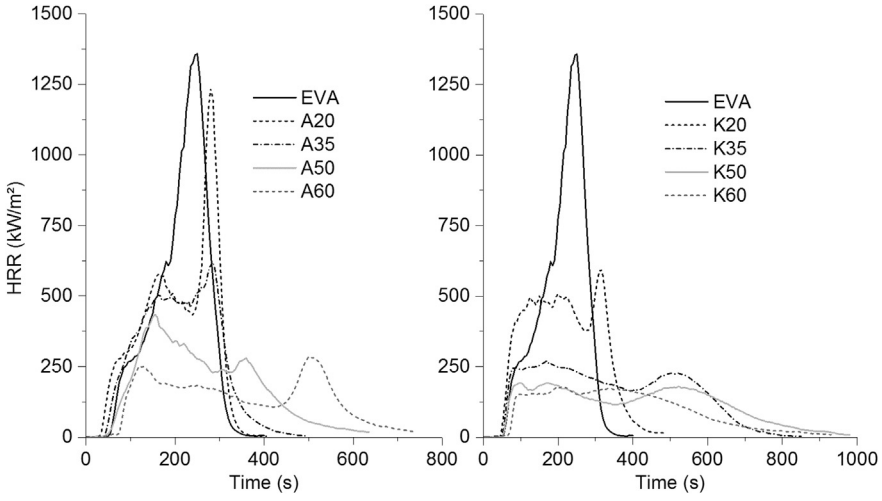

Fig. 1. Cone calorimeter tests for ATH and kaolinite EVA composites. Heat flux: 50 $kW.m^{-2}$.

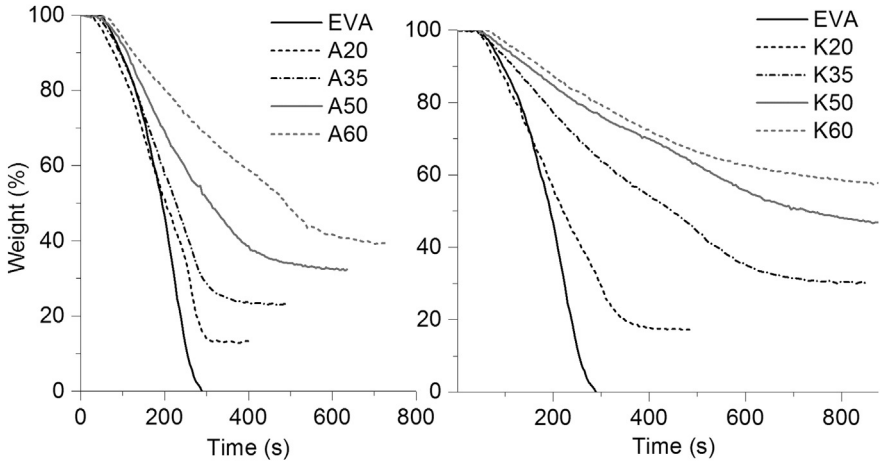

Fig. 2. Mass loss for ATH and kaolinite EVA composites obtained by cone calorimeter tests. Heat flux: 50 kW.m^{-2}.

residue content at flame out is higher for EVA/kaolinite than for EVA/ATH at similar filler content. For EVA/ATH composites, the residue contents at the flame out are equal to the theoretical values calculated considering no charring and complete decomposition of ATH into alumina. For EVA/kaolinite composites, the residue contents showed the same behavior as for EVA/ATH, except for K50 and K60 for which the residue are slightly higher than theoretical values considering no charring and complete decomposition of kaolinite. The good agreement between the experimental and theoretical residue contents for K20 and K35 confirms that water from kaolinite is released during the cone calorimeter test.

Time to ignition (TTI) is lower for all filled composites in comparison with neat polymer except for EVA filled with the highest contents of ATH or kaolinite. Some explanations have been proposed in the literature to explain the decrease of TTI in composites, including the catalytic effect of nanoparticles [2], the viscosity of the molten polymer [27] and, more recently, the absorption in-depth [28,29]. Absorption in-depth means that heat is not fully absorbed at the surface of the sample but partly penetrates into a layer with a finite thickness depending on the material. The heating rate of the sample surface (which controls the time to ignition) is faster or slower according to this thickness. The evolution of time to ignition showed an interesting behavior. The TTI values for kaolinite containing composites are higher than for ATH containing composites up to 50 wt%. At higher filler loading, the reverse tendency is observed. For ATH composites, water release is known to decrease the heating rate of the condensed phase (through the associated endothermic effect) and to dilute the fuel gas. Probably these phenomena are only effective at high ATH loading. For kaolinite containing composites, another explanation should be proposed since kaolinite releases only 14 wt% of water at temperature higher than the degradation temperature of EVA.

In the following, additional analyses are carried out to identify the modes-of-action of kaolinite. The EVA/ATH composites melted similarly as unfilled EVA during the fire test and showed a strong bubbling phenomenon even for 60 wt% loading. This bubbling was observed even during the pre-ignition period. On the contrary, the EVA/kaolinite composites did not exhibit such bubbling when the filler content exceeded 35 wt%.

Fig. 3 shows the evolution of the A35 and K35 samples at "Epiradiateur Test" which corresponds to a French standard (NFP 92−501) (see Fig. 4). In this test, a sample of 7 × 7 cm^2 is subjected to radiant heat emitted flux from a 500 W epiradiator (diameter 10 cm, made of opaque quartz). The irradiance can be estimated at

Table 2
Cone calorimeter results for ATH and Kaolinite EVA composites.

	ATH (%)	Kaolinite (%)	PHRR (kW.m^{-2})	TTI (s)	EHC (kJ/g)	THR (MJ.m^{-2})	Residue content (%)	Theoretical residue content[a] (%)
EVA	0	0	1504	48	35	154	0	0
A20	20	0	1032	29	32	138	13	13.1
A35	35	0	602	35	28	116	22.5	22.9
A50	50	0	411	47	26	107	32.2	32.7
A60	60	0	282	64	24	94	38.5	39.2
K20	0	20	596	37	33	136	17.6	17.0
K35	0	35	262	42	32	126	30.4	30.1
K50	0	50	199	46	32	107	45.1	43.1
K60	0	60	192	56	29	86	56.9	51.6

[a] Calculated as the sum of the mass loss at TGA of neat polymer and mass loss of the filler at 900 °C under air.

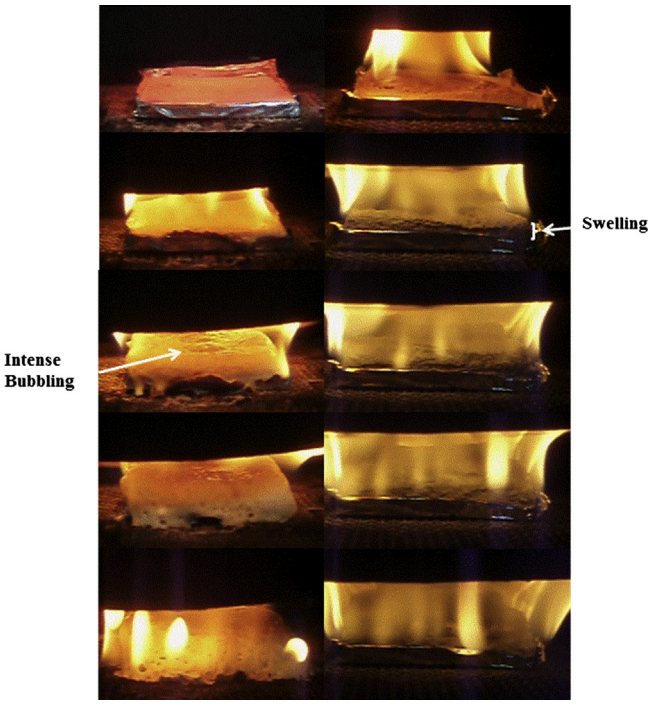

Fig. 3. Selected sequences of video images of Epiradiateur Test showing the intense bubbling for A35 (left) and the swelling behavior of K35 composites (right).

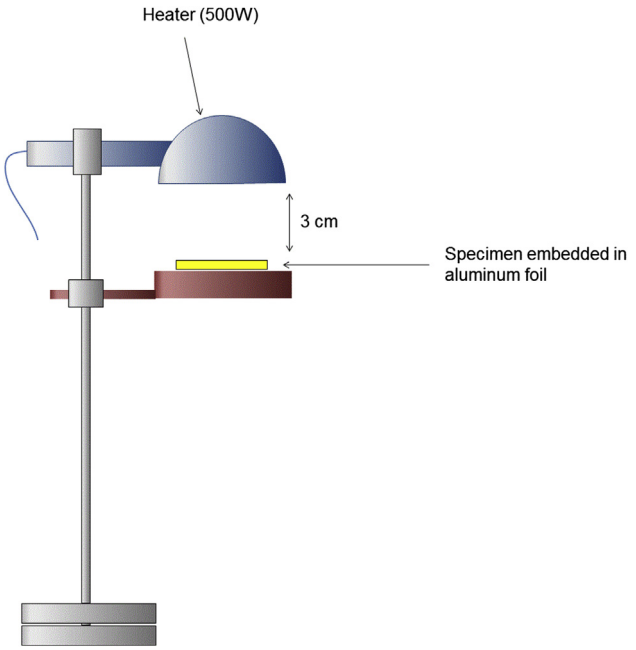

Fig. 4. Scheme of epiradiateur test.

around 35 kW/m^2. The epiradiator was used only to burn the samples without observing the French standard.

For the A35 composite, small bubbles burst at the surface of the sample, followed by ignition. After 100 s, the surface was covered by large bursting bubbles with vigorous bubbling. At the end of the test, no thick residue was found (Fig. 5a). All EVA/ATH samples exhibit thin, gray and non-cohesive residues. In the case of EVA/kaolinite, in the pre-ignition period, a black, protective and cohesive layer was observed which remained until the end of the test. Around 120 s, the sample started to swell. The final residue exhibited a thickness approximately equal to 8 mm (expansion ratio equal to 2) (Fig. 5b). For 35 wt% and more, the EVA/kaolinite composites show cohesive, expanded, and continuous residues without cracks.

Since kaolinite could limit bubbling, mass transfer from the pyrolysis front to the flame could be reduced. Moreover, the formation of a rigid and slightly expanded layer allows limiting not only mass transfer but also heat transfer from the flame to the underlying material: such barrier effect is well documented in literature for various nanocomposites [10,12,16,30,31], reducing the mass loss rate and the heat release rate. Moreover, the concept of mineral intumescence was proposed by Ferry et al. to account for the formation of expanded layers in EVA containing hydrated fillers and nanoparticles [31]. This effect seems to be consistent with the evolution of the mass loss rate curves obtained for kaolinite composites (Fig. 2).

The formation of a protective layer for EVA/kaolinite composites was confirmed by SEM analyses of the residues after cone calorimeter tests (Fig. 6). An orientation of the kaolinite particles along the surface of residue which form a mineral layer was noticed for K50. It should be noted that the formation of this protective layer was observed even during the pre-ignition period for all kaolinite composites. This effect was also reported in the literature for EVA/oMMT and EVA/oMMT/talc composites [1,5,8].

3.2. PCFC

Pyrolysis combustion flow calorimeter (PCFC) has been used to study the fire behavior of mg-sized samples [32–35]. The PCFC

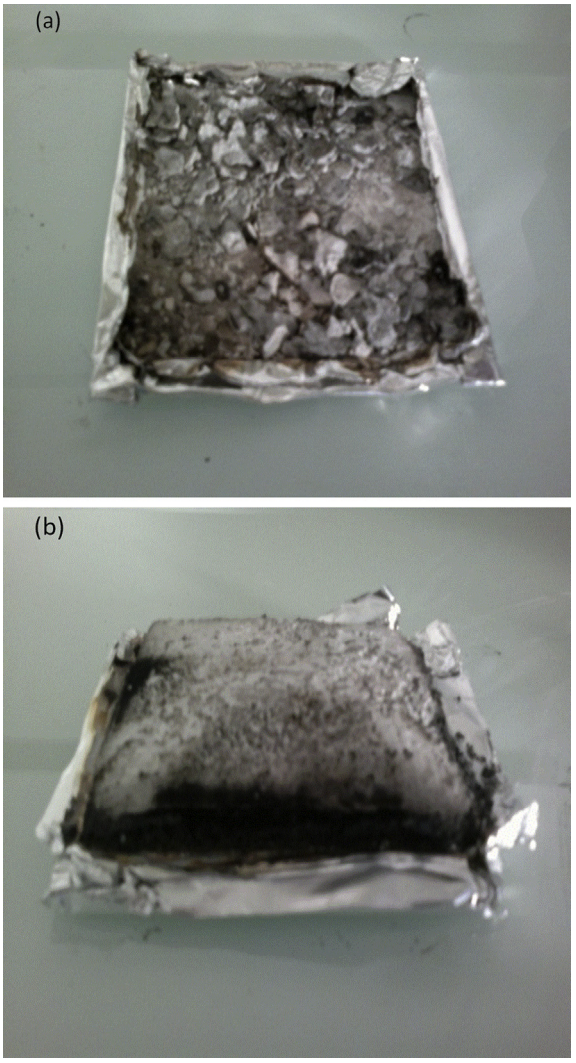

Fig. 5. Cone calorimeter residues of (a) A35 and (b) K35.

results are shown in Fig. 7. A decrease of HRR for both fillers is observed, being slightly greater for EVA/ATH, which could be due to the endothermic effect, despite it is limited in the case of EVA/kaolinite. Also, it should be noted that the degradation of the acetate group was accelerated as a function of kaolinite loading, as observed in TGA tests (see below). Moreover, the reduction in pHRR for all composites is less marked than in cone calorimeter test. Since it is known that PCFC test does not take into account physical effects like barrier effect, this one can be observed only for relatively big samples, but not for 1 - 2 mg-scale sample [32,35]. Using this assumption, we proposed in a previous study [35] a new method to evaluate the barrier effect by comparing the results of cone and PCFC tests. In the proposed method, two parameters are calculated: the ratio R_1 between HRC (Heat Release Capacity calculated as the ratio between pHRR and heating rate – 1 °C/s) of the composite and of the neat polymer in PCFC and the ratio R_2 between pHRR of the composite and of the neat polymer in cone. Then R_1 is plotted according to R_2 for different contents of mineral filler. The difference between the plotted points and the curve $X = Y$ depends on the barrier effect. Indeed an important shift ($R_1 >> R_2$) corresponds to a high barrier effect.

$$R_1 = \mathrm{HRC}_{\mathrm{composite}}/\ \mathrm{HRC}_{\mathrm{EVA}} \quad (1)$$

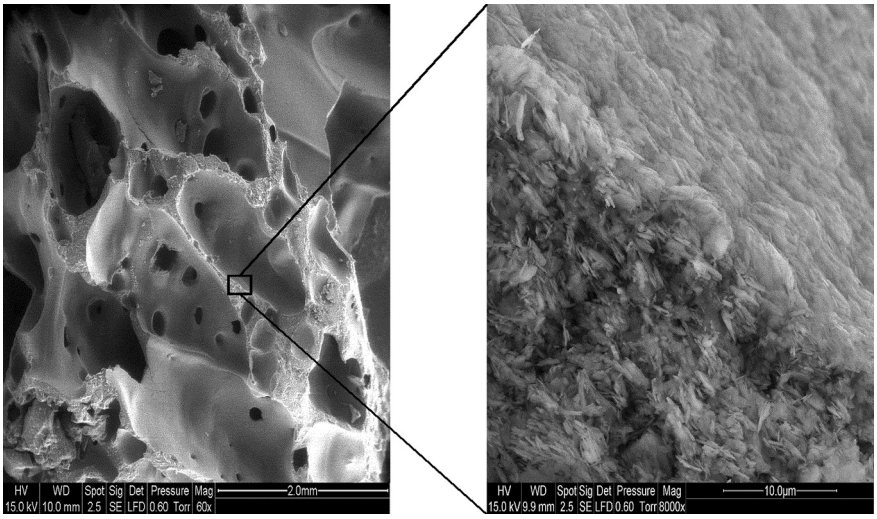

Fig. 6. SEM images of K50 cone calorimeter residues.

$$R_2 = \text{pHRR}_{\text{composite}}/\ \text{pHRR}_{\text{EVA}} \quad (2)$$

Fig. 8 plots R_1 vs. R_2. Results for EVA/kaolinite are shifted from the straight line $X = Y$, even for low filler contents. This deviation confirms our hypothesis for EVA/kaolinite composites: the heat and/or gas barrier effect is an important mode-of-action for the improvement of flame retardancy. It is more effective for EVA/kaolinite than for EVA/ATH composites.

3.3. *Thermal stability*

The thermal and thermo-oxidative degradation of EVA and EVA nanocomposites has been widely reported in the literature [1,2,8,9,11,12,14,31,36,37]. Thermal degradation of EVA takes place in two steps. The first one corresponds to a deacetylation, with the elimination of acetic acid between 300 and 400 °C. The second one is assigned to the degradation of the unsaturated products obtained by deacetylation (ethylene-co-acetylene [6]).

Thermogravimetric analyses were carried out in air and results are shown in Fig. 9. The deacetylation of EVA/kaolinite composites with the increase of kaolinite amount occurs at lower temperature as already pointed out from PCFC analyses. The presence of acid sites is known to have a catalytic effect [2,5] and could explain this phenomenon. In the case of organo-modified montmorillonite, Camino et al. [9] have ascribed this loss of acetic acid at lower temperatures to the presence of acid sites on the surface. To confirm this hypothesis, Costache et al. [38] carried out a series of experiments to modify the surface of a montmorillonite with a silane coupling agent (chlorotrimethylsilane). The authors showed that after this surface modification the nanocomposite degradation was the same as the neat polymer. They concluded that the acid sites of the clay surface have a catalytic effect in the degradation of EVA. For EVA/kaolinite composites, it seems that the same effect takes place. It should be noted that the cationic exchange capacity (and therefore the number of acid sites) of kaolinite is lower than montmorillonite. This could explain the lower influence observed on the degradation in comparison with montmorillonite. In the case of ATH composites, a first step of degradation takes place around 300 °C due to the presence of the mineral filler. This decomposition corresponds to the release of water.

For the second degradation step, kaolinite composites are slightly more stable than pure neat polymer and EVA/ATH composites. The temperature of this step under air or under nitrogen flow (Fig. 10) does not exhibit any difference for EVA/ATH. On the contrary, this step of degradation for EVA/kaolinite occurs at higher temperature only under air flow. This result leads to the conclusion

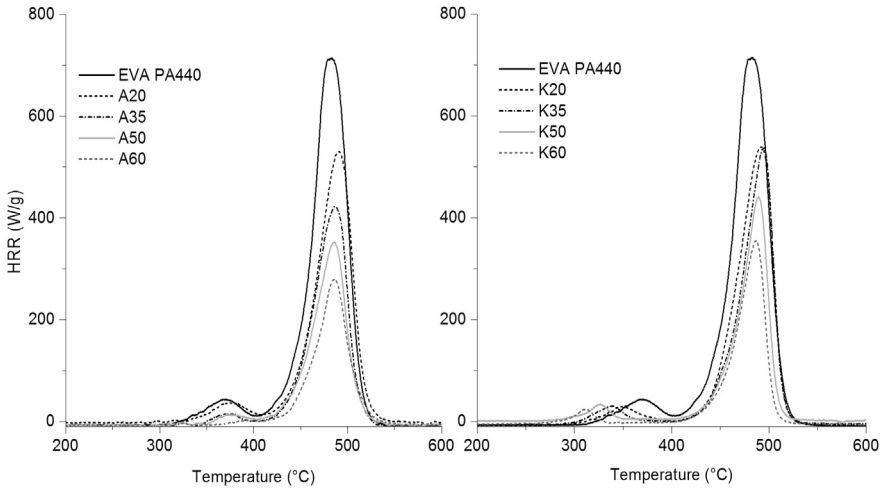

Fig. 7. PCFC curves of the ATH and kaolinite EVA composites.

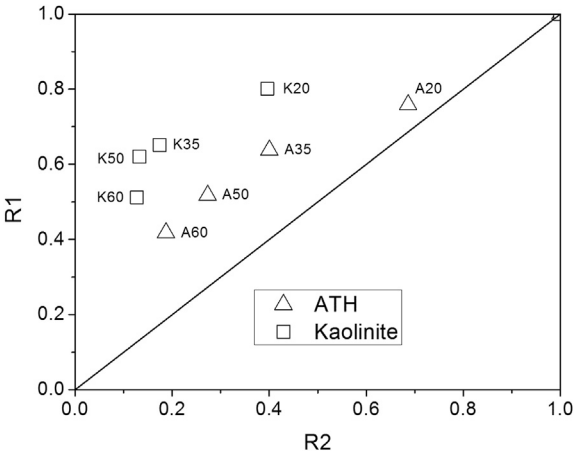

Fig. 8. R1 vs. R2 plots for ATH and kaolinite EVA composites.

that kaolinite promotes the formation of more stable products after deacetylation through crosslinking reactions involving the double bonds formed after acetic acid release. Another explanation is that kaolinite could act as oxygen barrier effect to delay the main degradation step of EVA. It should be noted that the last degradation step starting at about 500 °C observed in presence of kaolinite is due to the release of structural water from the mineral filler. Also, the TGA residue corresponds to the theoretical residue (calculated as the complete degradation of neat polymer and the complete release of water by kaolinite) of the filler without char formation.

3.4. Influence of viscosity on fire retardancy

As said above, the better performances of EVA/kaolinite composites in cone calorimeter test could be partly attributed to an efficient barrier effect. A specific aspect of the fire behavior of these composites is the disappearance of bubbling. ATH composites showed a strong bubbling, even in the pre-ignition period, which was not observed for kaolinite composites. This observation suggested an influence of the viscosity of different composites on cone calorimeter results. In order to determine the effect of the incorporation of both fillers on the rheology, apparent complex viscosity η^*, elastic modulus G' and tangent δ were measured. The storage modulus (G') shows the capability of the material to store energy that will be released after that the deformation is recovered. The loss modulus G'' is associated with the viscous energy dissipation and the ratio between G'' and G' is the loss tangent (tangent δ).

The viscosity properties are expected to have important effects on fire behavior. High viscosities should decrease the bubbles growth and their diffusion rate in the melt to the surface. These bubbles will burst at the surface and supply the flame with the fuel. Kashiwagi et al. [39] showed that an increase in the storage modulus (G') leads to a decrease in mass loss rate of polystyrene nanocomposites. The authors also showed that the rheology controlled the formation of a cohesive charred layer without cracks. Clerc et al. [5] showed that the swelling of EVA/talc composites could be dependent on the viscosity of the composites. The authors considered that viscosity could have an influence in the thickness of the residue and showed that the incorporation of more lamellar particles leads to a higher viscosity and a more swollen sample. Furthermore, the expansion of the residue, in the case of an intumescent system, is dependent on the viscosity of the material. In the case of organo-modified montmorillonites, when the content increases, the viscosity becomes too great to allow the expansion, which reduces swelling and leads to a poorer performance [6,39]. In the case of our samples, (Fig. 11), storage modulus increased for all formulations, in comparison to neat polymer, but this increase was higher for kaolinite composites. Generally, G' values increase with increasing shear rate [40]. As the mineral filler loading increases, the slope of G' vs. shear rate decreases. This is ascribed to the formation of a particle network structure in the blend (samples develop a more elastic character) [40]. Moreover, tangent δ shows a slightly different behavior. It remains almost constant for EVA/ATH composites but it decreases significantly for EVA/kaolinite composites, which indicates a more 'solid-like' state. It is well known that lamellar fillers tend to increase the viscosity of the composites [40], in comparison with lower aspect ratio particles. This explains why the composite viscosities with kaolinite are higher than with ATH.

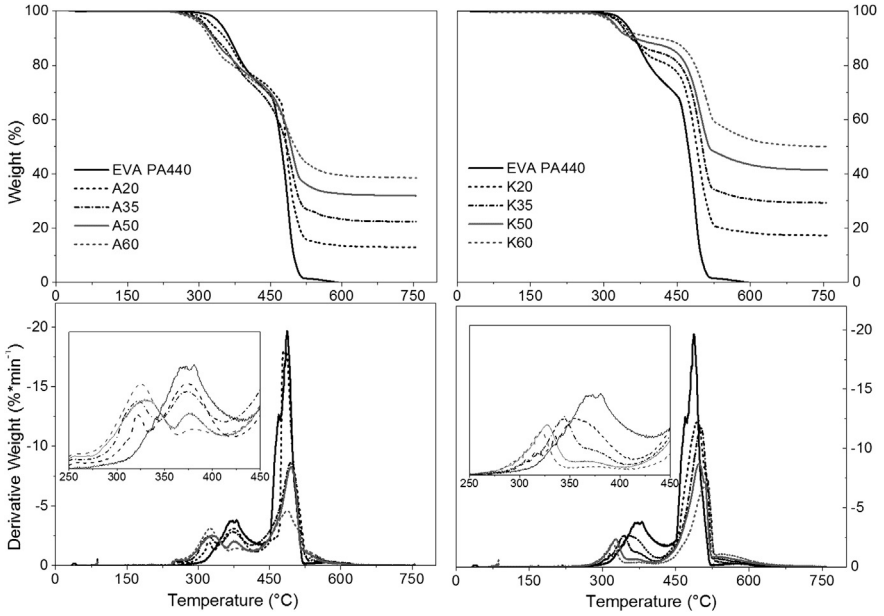

Fig. 9. TGA results in air of ATH and kaolinite EVA composites.

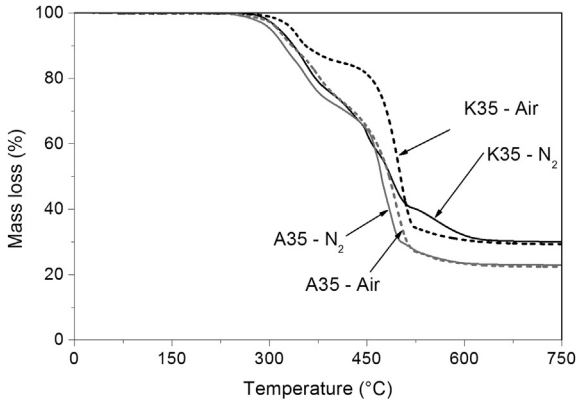

Fig. 10. TGA results of K35 and A35 under air and N_2.

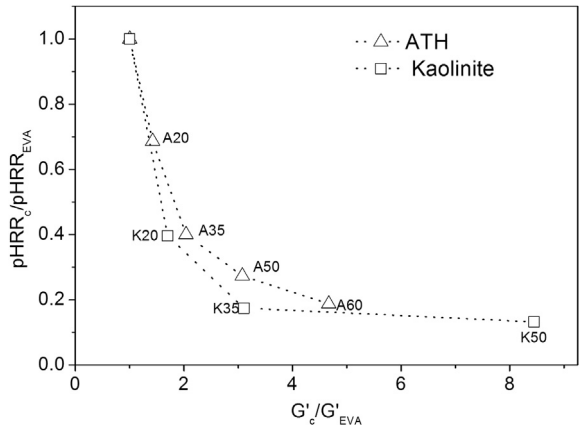

Fig. 12. Relative pHRR versus relative G' of the ATH and kaolinite composites.

Fig. 12 plots the relative pHRR versus the relative G' for EVA filled with kaolinite and ATH. Relative pHRR (respectively G') is calculated as the pHRR of the composite divided by the pHRR of pure EVA. It should be noticed that rheological measurements were recorded at 160 °C, while temperature in the condensed phase during cone calorimeter test increases from ambient to pyrolysis temperature of the polymer (i.e. approximately 450–500 °C for EVA). Nevertheless we assume that the hierarchy in viscosity between composites is qualitatively similar at processing temperature (160 °C) and during cone calorimeter test.

Two distinct tendencies could be observed. In the Regime 1, relative pHRR decreases quickly from 1 to 0.2 when relative elastic modulus increases from 1 to 5. From this value ($G'_c/G'_{EVA} \geq 5$) a second Regime is observed (Regime 2): relative pHRR remains almost constant close to 0.2, whatever the further increase of relative elastic modulus. This behavior supports the hypothesis that a more elastic composite (i.e. a higher G') could lead to an improved fire behavior by limiting bubbling, convection into the condensed phase and transfer of the pyrolysis gases to the flame. When these phenomena are limited enough (i.e. when G' becomes higher than a threshold value) the pHRR is stabilized and does not decrease anymore. To confirm our hypothesis, G' of additional composites at various filler contents (between 20 and 60 wt%) were compared. Filler type and contents as well as relative G′ and relative pHRR of all formulations are given in the appendix. Fig. 13 shows the plots of relative G′ vs. relative pHRR. All data and designation of fillers can be found in Appendix (Table A1 and A2). This result is particularly surprising because it would indicate that endothermic effect is not so efficient to decrease the pHRR: all the composites corresponding to the Regime II contain various contents of different fillers. Nevertheless, they exhibit all approximately the same pHRR.

Finally, this result allows specifying the barrier effect which was assumed to explain the better performances of EVA/kaolinite composites. Indeed, the addition of fillers to reduce the pHRR is only effective as long as the elasticity of the material is below a threshold value. Even if higher filler content should lead to a more insulating layer at the surface of the sample (because more mineral particles accumulate faster), pHRR remains constant. We believe that such results are more consistent with a barrier effect limiting the mass transfer from the pyrolysis front to the flame than with a heat shielding effect limiting the heat transfer from the flame to the underlying material.

4. Conclusions

The effect of incorporation of kaolinite was studied and compared with ATH. It was showed that the incorporation of kaolinite leads to better fire performances than ATH in cone calorimeter test. A better decrease in pHRR and increase in time to ignition was observed for formulations with kaolinite. The improved fire performance of EVA/kaolinite is mainly assigned to barrier effect closely related to its rheological behavior since the kaolinite promotes swelling and inhibits bubbling.

Thermal analysis showed that kaolinite seems to have also a catalytic effect in deacetylation of EVA, as was reported in the case of

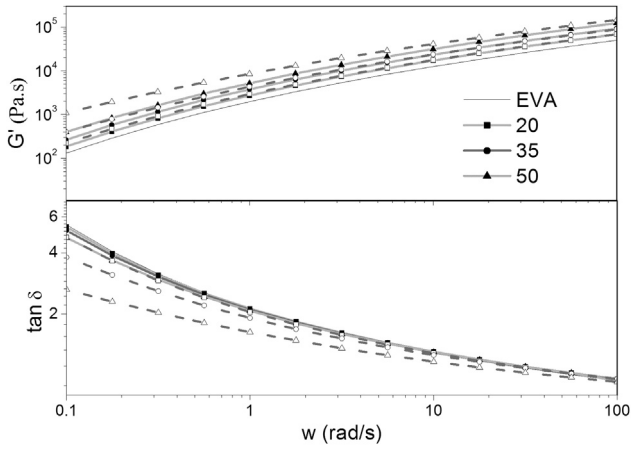

Fig. 11. Storage modulus (G') and tangent δ of ATH and kaolinite composites. Open symbols: EVA/Kaolinite; closed symbols: EVA/ATH.

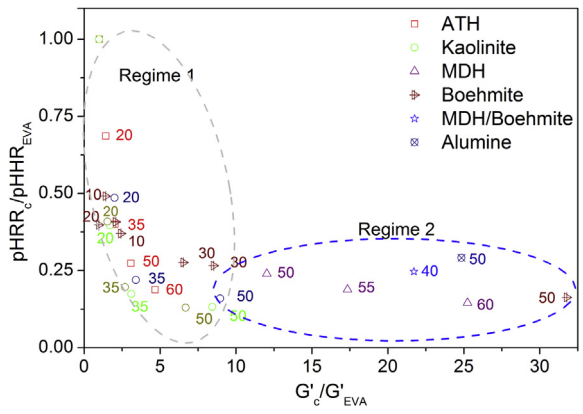

Fig. 13. Relative pHRR versus relative G' of different EVA composites.

other fillers. Also, it seems that kaolinite acts as an oxygen barrier, improving the stability of the main degradation steep of composites.

Rheological measurements allowed specifying the barrier effect. They showed that the composite viscosity has a major effect in the pHRR reduction, at least up to a certain value of G'. Above this threshold, pHRR decreases quickly when fillers are incorporated into EVA because the increase in elasticity limits bubbling and mass transfer from pyrolysis front to the flame. Below this threshold, pHRR remains constant and independent on the further increase in elasticity. The addition of more fillers does not lead to a further decrease in pHRR. In this case, the so-called barrier effect is not mainly heat shielding.

An optimum content of fillers could be defined, but such optimum is only valid for cone calorimeter tests. Indeed, endothermic effect and dilution of fuels by water seem very little effective in this test, contrarily to other fire tests (like Limiting Oxygen Index – LOI). For this reason, ATH is better than kaolinite to improve the LOI of EVA (29.5 for A60 and 22.5 for K60). Once again, this illustrates the lack of correlation between different fire tests [32,34,41,42].

Appendix

Table A1
Normalized values of G' and pHRR for different EVA composites.

Charge	Filler type	Filler content (%)	G'_c/G'_{EVA}	$pHRR_c/pHRR_{EVA}$
MDH	$Mg(OH)_2$	50	12.0	0.24
MDH	$Mg(OH)_2$	55	17.3	0.19
MDH	$Mg(OH)_2$	60	25.2	0.14
ATH-1	ATH	20	1.42	0.67
ATH-1	ATH	35	2.04	0.40
ATH-1	ATH	50	3.10	0.27
ATH-2	ATH	50	27.1	0.37
ATH-3	ATH	50	21.3	0.18
K1	Kaolinite	20	1.70	0.40
K1	Kaolinite	35	3.10	0.17
K1	Kaolinite	50	8.45	0.13
K2	Kaolinite	20	2.0	0.48
K2	Kaolinite	35	3.4	0.22
K2	Kaolinite	50	8.9	0.16
K3	Kaolinite	20	1.5	0.41
K3	Kaolinite	35	2.7	0.20
K3	Kaolinite	50	6.6	0.13
Alumina	Alumina	50	24.9	0.39
B1	Boehmite	50	31.8	0.35
B2	Boehmite	10	0.9	0.4
B2	Boehmite	20	2.4	0.37
B2	Boehmite	30	6.5	0.28
B3	Boehmite	10	1.4	0.39
B3	Boehmite	20	2.0	0.40
B3	Boehmite	30	8.5	0.26
MDH/B1	$Mg(OH)_2$/boehmite	20/20	21.7	0.25

Table A2
Characteristics of different fillers used.

Filler	Reference	d_{50} (μm)	Specific surface area ($m^2.g^{-1}$)
MDH	Magnifin H10 (Albemarle)	0.65–0.95	9–11
ATH-1	Apyral 22 (Nabaltec)	2	12
ATH-2	ON313 (Albemarle)	12	
ATH-3	Apyral 24 (Nabaltec)	8	2.4
Kaolinite K1	Paralux (Imerys)	0.8	14.2
Kaolinite K2	Not Commercial	0.2	16
Kaolinite K3	Paraplate (Imerys)	2	8
B1	Apyral AOH20 (Nabaltec)		2
B2	CAM 9010 (Saint-Gobain)	0.1–0.15	130
B3	CAM 9060 (Saint-Gobain)	0.08–0.1	160
Alumina	Prolabo	28	

References

[1] Riva A, Zanetti M, Braglia M, Camino G, Falqui L. Thermal degradation and rheological behaviour of EVA/montmorillonite nanocomposites. Polym Degrad Stab 2002;77:299–304.
[2] Zanetti M, Camino G, Thomann R, Mülhaupt R. Synthesis and thermal behaviour of layered silicate-EVA nanocomposites. Polymer 2001;42:4501–7.
[3] Riva A, Camino G, Fomperie L, Amigouët P. Fire retardant mechanism in intumescent ethylene vinyl acetate compositions. Polym Degrad Stab 2003;82:341–6.
[4] Cross MS, Cusack PA, Hornsby PR. Effects of tin additives on the flammability and smoke emission characteristics of halogen-free ethylene-vinyl acetate copolymer. Polym Degrad Stabil 2003;79:309–18.
[5] Clerc L, Ferry L, Leroy E, Lopez-Cuesta JM. Influence of talc physical properties on the fire retarding behaviour of (ethylene-vinyl acetate copolymer/magnesium hydroxide/talc) composites. Polym Degrad Stab 2005;88:504–11.
[6] Zanetti M, Kashiwagi T, Falqui L, Camino G. Cone calorimeter combustion and gasification studies of polymer layered silicate nanocomposites. Chem Mater 2002;14:881–7.
[7] Camino G, Maffezzoli A, Braglia M, De Lazzaro M, Zammarano M. Effect of hydroxides and hydroxycarbonate structure on fire retardant effectiveness and mechanical properties in ethylene-vinyl acetate copolymer. Polym Degrad Stab 2001;74:457–64.
[8] Duquesne S, Jama C, Le Bras M, Delobel R, Recourt P, Gloaguen J. Elaboration of EVA–nanoclay systems—characterization, thermal behaviour and fire performance. Compos Sci Technol 2003;63:1141–8.
[9] Camino G, Sgobbi R, Zaopo A, Colombier S, Scelza C. Investigation of flame retardancy in EVA. Fire Mater 2000;24:85–90.
[10] Lv J, Liu W. Flame retardancy and mechanical properties of EVA nanocomposites based on magnesium hydroxide nanoparticles/microcapsulated red phosphorus. J Appl Polym Sci 2007;105:333–40.
[11] Durin-France A, Ferry L, Lopez Cuesta J-M, Crespy A. Magnesium hydroxide/zinc borate/talc compositions as flame-retardants in EVA copolymer. Polym Int 2000;49:1101–5.
[12] Beyer G. Flame retardant properties of EVA-nanocomposites and improvements by combination of nanofillers with aluminium trihydrate. Fire Mater 2001;25:193–7.
[13] Bertini F, Canetti M, Audisio G, Costa G, Falqui L. Characterization and thermal degradation of polypropylene-montmorillonite nanocomposites. Polym Degrad Stab 2006;91:600–5.
[14] Costache MC, Heidecker MJ, Manias E, Camino G, Frache A, Beyer G, et al. The influence of carbon nanotubes, organically modified montmorillonites and layered double hydroxides on the thermal degradation and fire retardancy of polyethylene, ethylene-vinyl acetate copolymer and polystyrene. Polymer 2007;48:6532–45.
[15] Davis RD, Gilman JW, VanderHart DL. Processing degradation of polyamide 6/montmorillonite clay nanocomposites and clay organic modifier. Polym Degrad Stab 2003;79:111–21.
[16] Gilman J. Flammability and thermal stability studies of polymer layered-silicate (clay) nanocomposites. Appl Clay Sci 1999;15:31–49.
[17] Almeras X, Le Bras M, Hornsby P, Bourbigot S, Marosi G, Keszei S, et al. Effect of fillers on the fire retardancy of intumescent polypropylene compounds. Polym Degrad Stabil 2003;82:325–31.
[18] Marney DCO, Russell LJ, Wu DY, Nguyen T, Cramm D, Rigopoulos N, et al. The suitability of halloysite nanotubes as a fire retardant for nylon 6. Polym Degrad Stab 2008;93:1971–8.
[19] Hull TR, Witkowski A, Hollingbery L. Fire retardant action of mineral fillers. Polym Degrad and Stab 2011;96:1462–9.
[20] Van Olphen H. An introduction to clay colloid chemistry: for clay technologists, geologists, and soil scientists. New York: Interscience Publishers; 1965.
[21] Grim RE. Clay mineralogy. New York: McGraw-Hill; 1968.
[22] Wang L, Xie X, Su S, Feng J, Wilkie CA. A comparison of the fire retardancy of poly(methyl methacrylate) using montmorillonite, layered double hydroxide and kaolinite. Polym Degrad Stab 2010;95:572–8.
[23] Vahabi H, Batistella MA, Otazaghine B, Longuet C, Ferry L, Sonnier R, et al. Influence of a treated kaolinite on the thermal degradation and flame retardancy of poly(methyl methacrylate). Appl Clay Sci 2012;70:58–66.
[24] Genovese A, Shanks R. Fire performance of poly(dimethyl siloxane) composites evaluated by cone calorimetry. Compos Part A Appl Sci Manuf 2008;39:398–405.
[25] Swoboda B, Leroy E, Lopez-Cuesta JM, Artigo C, Petter C, Sampaio Ch. In: Richard Hull T, Kandola Baljinder K, editors. Fire retardancy of polymers – new strategies and mechanisms, vol. 5. RSC Publishing; 2008. pp. 59–73.
[26] Vaughan F. Energy changes when Kaolin minerals are heated. Clay Miner 1955;2:265–74.
[27] Hull TR, Stec AA, Nazare S. Fire retardant effects of polymer nanocomposites. J Nanosci Nanotechnol 2009;9:4478–86.
[28] Delichatsios MA, Zhang J. An alternative way for the ignition times for solids with radiation absorption in-depth by simple asymptotic solutions. Fire Mater 2012;36:41–7.
[29] Fina A, Feng J, Cuttica F. In-depth radiative heat transmittance through polypropylene/nanoclay composites. Polym Degrad Stab 2013;98:1030–5.
[30] Lewin M, Pearce EM, Levon K, Mey-Marom A, Zammarano M, Wilkie CA, et al. Nanocomposites at elevated temperatures: migration and structural changes. Polym Adv Technol 2006;17:226–34.

[31] Ferry L, Gaudon P, Leroy E, Lopez-Cuesta JM. Fire retardancy of polymers: new applications of mineral fillers fire retardancy of polymers: the use of mineral fillers in micro and nano-composites. R Soc Chem 2005;22:345–58.
[32] Schartel B, Pawlowski KH, Lyon RE. Pyrolysis combustion flow calorimeter: a tool to assess flame retarded PC/ABS materials? Thermochimica Acta 2007;462:1–14.
[33] Lyon RE, Walters RN. Pyrolysis combustion flow calorimetry. J Anal Appl Pyrol 2004;71:27–46.
[34] Lyon RE, Walters RN, Stoliarov II S. Screening flame retardants for plastics using microscale combustion calorimetry. Polym Eng Sci 2007;47:1501–10.
[35] Sonnier R, Ferry L, Longuet C, Laoutid F, Friederich B, Laachachi A, et al. Combining cone calorimeter and PCFC to determine the mode of action of flame-retardant additives. Polym Adv Technol 2011;22:1091–9.
[36] Camino G, Costa L, Martinasso G. Intumescent fire-retardant systems. Polym Degrad Stab 1989;23:359–76.
[37] Le Bras M, Bourbigot S, Revel B, Bras MLE. Comprehensive study of the degradation of an intumescent EVA-based material during combustion. J Mater Sci 1999;4:5777–82.
[38] Costache MC, Jiang DD, Wilkie CA. Thermal degradation of ethylene-vinyl acetate copolymer nanocomposites. Polymer 2005;46:6947–58.
[39] Kashiwagi T, Mu M, Winey K, Cipriano B, Raghavan SR, Pack S, et al. Relation between the viscoelastic and flammability properties of polymer nanocomposites. Polymer 2008;49:4358–68.
[40] Shenoy AV. Rheology of filled polymer systems. AA Dordrecht: Kluwer Academin Publishers; 1999.
[41] Cogen JM, Lin TS, Lyon RE. Correlations between pyrolysis combustion flow calorimetry and conventional flammability tests with halogen-free flame retardant polyolefins compounds. Fire Mater 2009;33:33–50.
[42] Morgan AB, Galaska M. Microcombustion calorimetry as a tool for screening flame retardancy in epoxy. Polym Adv Technol 2008;19:530–46.